

Broadband Omnidirectional Dual-Polarized Antenna using Multimode Coupling in Wi-Fi 6 Routers

Xuxuan Lin ⁽¹⁾, Yongjian Zhang ⁽¹⁾, and Yue Li ^{(1), (2), (3)}

(1) Department of Electronic Engineering, Tsinghua University, Beijing, 100084, China (lyee@tsinghua.edu.cn)

(2) Beijing National Research Center for Information Science and Technology, Beijing, 100084, China

(3) State Key laboratory of Space Network and Communications, Tsinghua University, Beijing, 100084, China

Abstract—This paper proposes a broadband omnidirectional dual-polarized antenna for Wi-Fi 6 applications in routers. For horizontal polarization, an open-ended cavity is excited at its TE_{1/2,0,0} and TE_{1/2,0,2} modes to provide horizontally polarized omnidirectional radiation. These two resonant modes are coupled by loading shorting vias into the cavity, broadening the operating bandwidth. For vertical polarization, two H-shaped slots carved on the cavity are excited to form a folded equivalent magnetic current, enabling omnidirectional vertically polarized radiation. Experimental results show that the proposed antenna achieves broad bandwidths of 4.94–6.25 GHz for horizontal polarization and 5.15–5.85 GHz for vertical polarization. The measured gain variations are lower than 5.0 dB and 3.2 dB for horizontal and vertical polarizations, respectively. With the compact volume of 16.5×6.5×100 mm³ (0.30λ₀×0.12λ₀×1.83λ₀), the proposed antenna can be integrated into routers, making it a promising candidate for applications in wireless router systems.

I. INTRODUCTION

With the rapid advancement of wireless communication technologies, Wi-Fi 6 has developed numerous application scenarios due to its stable and high-performance Internet connectivity capabilities [1], [2]. As a critical component in communication systems utilizing the Wi-Fi 6 standard, router antennas are required to provide wide bandwidth to enhance throughput rates [3], [4], [5], omnidirectional radiation patterns to ensure user coverage [6], [7] and dual-polarized operation to avoid polarization mismatch [8], [9]. However, it is a challenge to achieve these characteristics simultaneously in the limited space, which restricts the widespread adoption of Wi-Fi 6.

Recently, omnidirectional dual-polarized antennas have been widely studied and used by two main approaches. The first approach combines elements with vertical and horizontal polarizations to form a circular array. This method provides excellent omnidirectional radiation and wide bandwidth, but it often results in a large volume, making it difficult to integrate into routers [10], [11], [12], [13]. The second approach is based on cavity structures, in which the horizontal polarization modes are excited, and vertical polarization is provided through methods such as etching slots [14], [15], [16], [17]. Antennas designed by this method have a compact structure, but the bandwidth is generally narrow, making it unable to cover the operating frequency of Wi-Fi 6.

In this work, a broadband omnidirectional dual-polarized antenna is proposed for Wi-Fi 6 router applications. For horizontal polarization, the 0th and 2nd modes of the cavity are

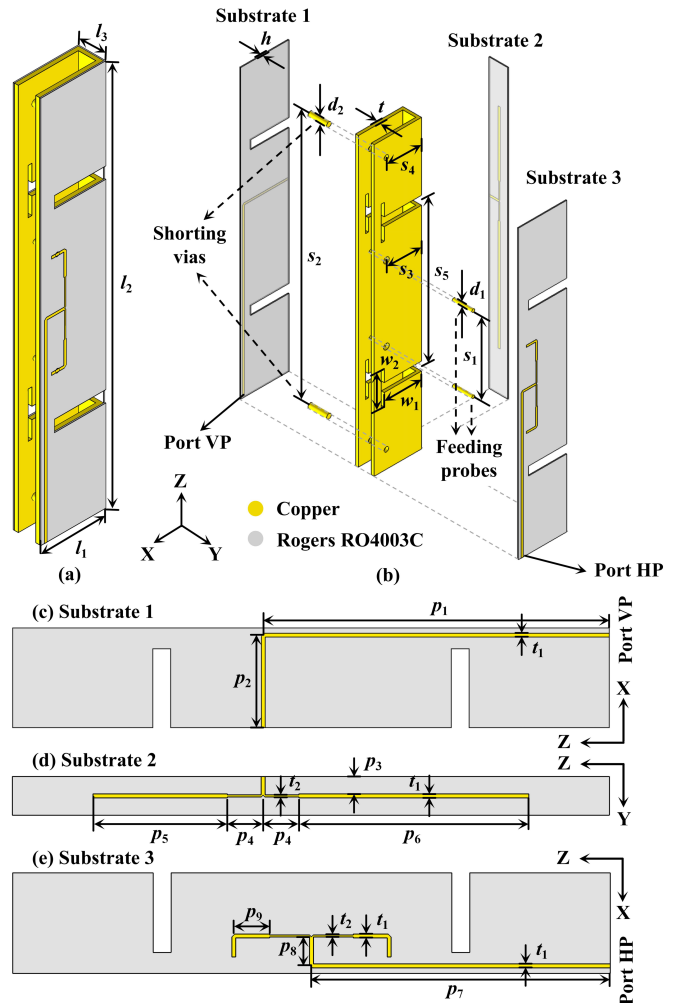


Figure 1. Geometry and dimensions of the proposed antenna. (a) Perspective view. (b) Exploded view. Feeding networks for (c) (d) vertical polarization and (e) horizontal polarization.

excited, and multimode coupling is achieved to extend the bandwidth. For vertical polarization, two slots are etched on the cavity to form a 2-element array with vertical polarization. A prototype was fabricated for testing, and experimental results show that the proposed antenna achieves omnidirectional dual-polarized radiation in the 5-GHz band of Wi-Fi 6, meeting the application requirements of Wi-Fi 6 routers.

TABLE I. DETAILED DIMENSIONS (UNIT: MM).

Parameters	l_1	l_2	l_3	d_1	d_2	t
Size	16.5	100	6.5	1.6	1	1
Parameters	s_1	s_2	s_3	s_4	s_5	p_1
Size	26	88	12.25	12.25	50	58
Parameters	p_2	p_3	p_4	p_5	p_6	p_7
Size	15.55	3.25	6	22.5	38.5	50
Parameters	p_8	p_9	w_1	w_2	t_1	t_2
Size	4.82	6	13	11.7	0.658	0.347

II. ANTENNA CONFIGURATION AND OPERATING MODES

A. Antenna Configuration

Fig. 1 shows the geometry of the proposed antenna, in which yellow represents copper and gray denotes Rogers RO4003C dielectric substrate ($\epsilon_r = 3.55$ and $\tan \delta = 0.0027$). The copper cavity is open-ended with a sidewall thickness of $t = 1$ mm. As shown in Fig. 1(b), three dielectric substrates are attached to the outer surface of the sidewalls of the cavity. For horizontal polarization, the operating modes are excited through a two-way power divider with two probes. To achieve multimode coupling for a wide frequency band, two shorting vias are loaded into the cavity symmetrically. For vertical polarization, two H-shaped folded slots are etched on the cavity. A two-way power divider with unequal-length branches is employed to excite vertically polarized omnidirectional radiation. The power divider provides outputs with opposite phases, ensuring that the fields excited in the two slots are in-phase. To reduce the influence of the substrates on vertically polarized radiation, the substrates covering the main structure of the folded slots are removed. Detailed dimensions are provided in Table I.

B. Multimode Coupling for Horizontal Polarization

Fig. 2 shows the operating modes of horizontal polarization in the proposed antenna, in which the dielectric substrates and feeding networks are omitted for clear illustration. As the size of the cavity along the Z-axis increases, the resonant frequency of the $TE_{1/2,0,2}$ mode decreases. By adjusting the dimensions of the cavity, the $TE_{1/2,0,0}$ mode and $TE_{1/2,0,2}$ mode can be excited within adjacent frequency ranges, which makes multimode coupling possible. The $TE_{1/2,0,0}$ mode represents a uniform electric field distribution along the Z-axis, while the $TE_{1/2,0,2}$ mode indicates an electric field with one-wavelength distribution along the Z-axis.

When no shorting vias are loaded into the cavity, the resonant frequencies of the two modes are separated, each forming a narrow operating bandwidth. When shorting vias are loaded, the resonant frequencies of the two modes shift to higher frequencies. Due to the stronger electric field of the $TE_{1/2,0,2}$ mode at the position of the vias, and the relatively weaker electric field of the $TE_{1/2,0,0}$ mode, the resonant frequency of $TE_{1/2,0,0}$ shifts more significantly, while that of $TE_{1/2,0,2}$ shifts less. This results in the coupling of the two operating bands into a wider bandwidth.

As shown in Fig. 2(a), the equivalent magnetic current formed by the $TE_{1/2,0,0}$ mode is vertically in-phase, providing

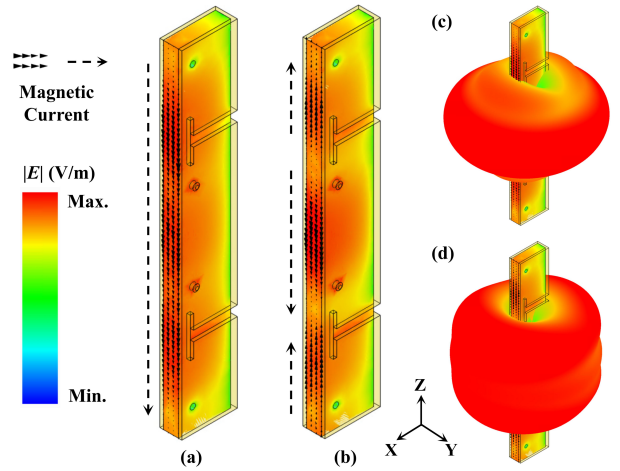


Figure 2. The electric field and equivalent magnetic current distribution at (a) $TE_{1/2,0,0}$ mode, (b) $TE_{1/2,0,2}$ mode and 3D radiation patterns at (c) $TE_{1/2,0,0}$ mode, (d) $TE_{1/2,0,2}$ mode.

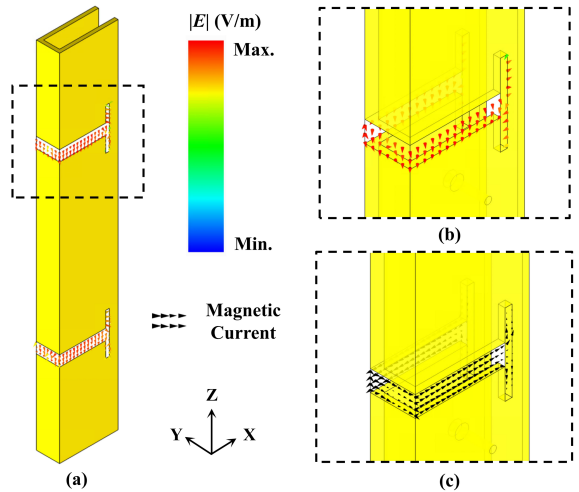


Figure 3. The operating mode of vertically polarized omnidirectional radiation. (a) The in-phase electric field in the two slots. The (b) electric field and (c) equivalent magnetic current distribution in a single slot.

omnidirectional horizontally polarized radiation with high aperture efficiency. As shown in Fig. 2(b), the equivalent magnetic current of the $TE_{1/2,0,2}$ mode has an out-of-phase distribution. However, because this mode is coupled with the $TE_{1/2,0,0}$ mode, it still exhibits an omnidirectional radiation pattern in the azimuthal plane with relatively high gain.

C. 2-Element Slot Array for Vertical Polarization

Fig. 3 illustrates the operating mode of vertical polarization in the proposed antenna, in which the dielectric substrates and feeding networks are omitted for clear illustration. As shown in Fig. 3(a), for a single H-shaped folded slot, the microstrip feedline is fed at the midpoint of the short edge, symmetrically exciting the electric fields in both halves of the slot, and the electric fields are in-phase in the slot. Therefore, the electric field in the slot can be equivalently represented as a continuous magnetic current along the slot, as shown in Fig. 3(c). This equivalent magnetic current can be regarded as a loop with a small gap, which will provide a radiation pattern that is close to

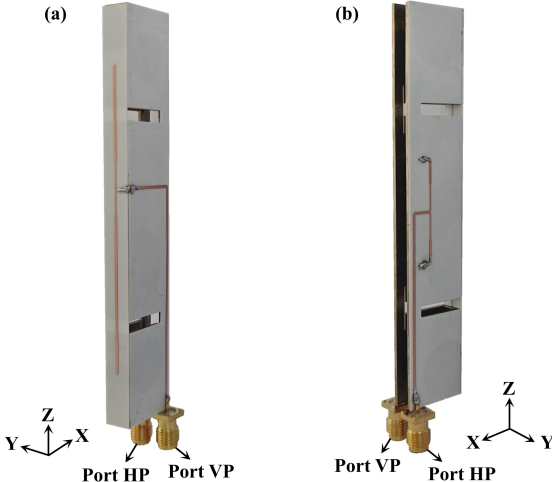


Figure 4. Photograph of the prototype of the proposed antenna. View from the feeding networks for (a) vertical and (b) horizontal polarizations.

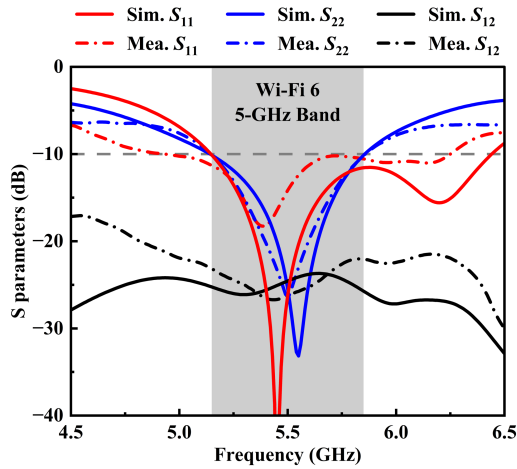


Figure 5. Simulated and measured S-parameters of the proposed antenna. Port 1 refers to Port HP, port 2 refers to Port VP.

omnidirectional in the azimuthal plane.

To enhance the gain and aperture efficiency of the vertical polarization, the proposed antenna introduces two of the aforementioned vertically polarized elements. As a 2-element array, reducing the spacing s_5 between the slots can reduce the grating lobes, and the influence on the horizontal polarization should be minimized. Therefore, the distance between the two elements along the Z-axis is optimized to be $s_5 = 50$ mm. At this distance, impedance matching is achieved, and the grating lobes of the array radiation are suppressed.

III. FABRICATION AND MEASUREMENT

To validate the design of the proposed broadband omnidirectional dual-polarized antenna, a prototype was fabricated, whose photograph is shown in Fig. 4. The cavity was fabricated via computer numerical control (CNC) machining using H59 brass as the material. The dielectric substrates were fabricated by the printed circuit board (PCB) process, and the material is Rogers RO4003C ($\epsilon_r = 3.55$ and $\tan \delta = 0.0027$).

Fig. 5 shows the measured S-parameters of the proposed antenna, which was obtained with an Agilent N9917A vector network analyzer. The measured impedance bandwidths for the

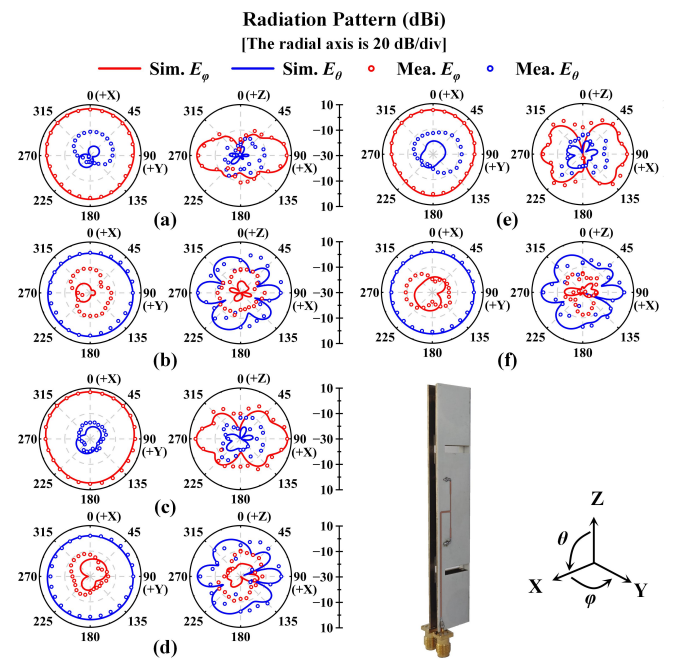


Figure 6. Simulated and measured radiation patterns in the XOY and XOZ planes of the proposed antenna. Feeding through Port HP at (a) 5.2, (c) 5.5, (e) 5.8 GHz, and feeding through Port VP at (b) 5.2, (d) 5.5, (f) 5.8 GHz.

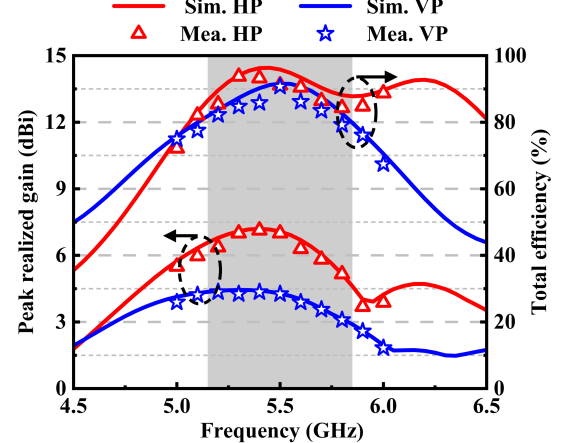


Figure 7. Simulated and measured total efficiencies and peak realized gains of the proposed antenna.

Port HP and Port VP feedings are 4.94–6.25 GHz (23.4%) and 5.15–5.85 GHz (12.7%), respectively. The two resonant modes observed in the measured results align with the simulation results and the overlapping frequency band covers the 5-GHz band of Wi-Fi 6 (highlighted with a gray background in Fig. 5). In the 5-GHz band of Wi-Fi 6, the transmission coefficient is lower than -22 dB, showing the high polarization isolation of the proposed antenna.

The radiation patterns of the proposed antenna were measured in a standard microwave anechoic chamber. As shown in Fig. 6, the radiation patterns of the proposed antenna in the azimuthal plane, i.e., the XOY plane, are omnidirectional. The measured results indicate that the gain variation of the proposed antenna in the azimuthal plane is lower than 5.0 dB and 3.2 dB when fed through Port HP and Port VP, respectively, meeting the requirements for practical router applications. Grating lobes

TABLE II. COMPARISONS WITH ODP ANTENNAS IN THE LITERATURE.

Ref.	Size (λ_0^3)	Overlapping BW ^a (GHz)	Gain for HP/VP (dBi)	GV ^b for HP/VP (dB)
[15]	$0.34 \times 0.13 \times 0.24$	2.40–2.48 (3.3%)	1.8/1.4	3.0/3.5
[16]	$\pi \times 0.07^2 \times 0.60$	0.83–0.92 (10.3%)	2.3/3.1	3.3/0.8
[17]	$0.25 \times 0.07 \times 0.25$	2.45–2.47 (0.8%)	0.8/2.2	3.7/3.7
T.W.	0.30×0.12×1.83	5.15–5.85 (12.7%)	7.4/4.4	5.0/3.2

^a “BW” represents “bandwidth”.^b “GV” represents “gain variation in the azimuthal plane”.

are observed in the XOZ plane. For horizontal polarization, the grating lobes are generated by the 2nd mode of the cavity. For vertical polarization, the grating lobes arise due to the relatively large spacing between the array elements. Since the grating lobes are relatively low in the desired band, the radiation is primarily distributed in the azimuthal plane, meeting the design requirements.

Fig. 7 shows the total efficiencies and peak realized gains of the proposed antenna, which can be calculated from the measured radiation patterns. The measured results show a high consistency with the simulation results. The measured results indicate that in the 5-GHz band of Wi-Fi 6, an efficiency of higher than 81.0% and a peak realized gain of 7.4 dBi are achieved when fed through Port HP, while an efficiency of higher than 77.1% and a gain of 4.4 dBi are achieved when fed through Port VP. Therefore, the radiation performance of the proposed antenna has been validated, and it meets the requirements for Wi-Fi 6 router antennas.

To highlight the merits of the proposed antenna, Table II presents a comparative analysis with other omnidirectional dual-polarized antennas. Compared to the previous designs, the proposed antenna offers a broader bandwidth while maintaining a small cross-sectional area.

IV. CONCLUSION

In this paper, a broadband antenna with dual-polarized omnidirectional radiation patterns suitable for routers is proposed. The proposed antenna has dimensions of $16.5 \times 6.5 \times 100$ mm³, and its small cross-sectional area allows it to be used as an external antenna for routers. To broaden the bandwidth for horizontal polarization, the method of multimode coupling is employed, and the bandwidth for horizontal polarization is extended to 4.94–6.25 GHz (23.4%). The slots etched on the cavity provides vertically polarized omnidirectional radiation, and the gain and aperture efficiency are enhanced through array configuration. The proposed antenna achieves gain variation of lower than 5.0 dB for horizontal polarization and lower than 3.2 dB for vertical polarization in the desired band, meeting the requirements of application. With the advantages of compact size, wide bandwidth and omnidirectional radiation, the proposed antenna presents a promising solution for Wi-Fi 6 router antennas.

ACKNOWLEDGMENT

This work was supported by the National Natural Science Foundation of China under Grant U22B2016 and the National

Key Research and Development Program of China under Grant 2021YFA0716601, in part by China Postdoctoral Science Foundation under Grant GZB20240334 and 2024M751678.

REFERENCES

- [1] M. S. Afiaqui, E. Garcia-Villegas, and E. Lopez-Aguilera, “IEEE 802.11ax: Challenges and Requirements for Future High Efficiency WiFi,” *IEEE Wireless Commun.*, vol. 24, no. 3, pp. 130–137, Jun. 2017.
- [2] D.-J. Deng, K.-C. Chen, and R.-S. Cheng, “IEEE 802.11ax: Next generation wireless local area networks,” in *Proc. Int. Conf. Heterogeneous Netw. Quality, Rel. Secur. Robustness*, Rhodes, Greece, Aug. 2014, pp. 77–82.
- [3] A. Kou, J. Chen, Z. Lin, T. Ding, C. -Z. Han and Y. Wei, “A Broadband Back-Cavity Antenna for Wi-Fi 6/6E Application,” in *Proc. Int. Conf. Microw. Millimeter Wave Technol.*, Qingdao, China, May 2023, pp. 1–2.
- [4] M. Chen, L. Chang, and A. Zhang, “Wideband Antenna Pairs Consisting of E-/M-Coupling Frame Monopoles and M-/E-Coupling Back Cover Patches for Mobile Terminal Applications,” *IEEE Trans. Antennas Propag.*, vol. 72, no. 2, pp. 1308–1318, Feb. 2024.
- [5] J. Deng, S. Hou, L. Zhao and L. Guo, “Wideband-to-Narrowband Tunable Monopole Antenna With Integrated Bandpass Filters for UWB/WLAN Applications,” *IEEE Antennas Wireless Propag. Lett.*, vol. 16, pp. 2734–2737, 2017.
- [6] H. Chen, X. Yang, Y. Z. Yin, S. T. Fan, and J. J. Wu, “Triband Planar Monopole Antenna With Compact Radiator for WLAN/WiMAX Applications,” *IEEE Antennas Wireless Propag. Lett.*, vol. 12, pp. 1440–1443, 2013.
- [7] C.-K. Lin, D.-B. Lin, and C.-K. Yu, “A Compact Multiband Monopole Antenna for Wi-Fi Applications,” in *Proc. IEEE Int. Workshop Antenna Technol.*, Sendai, Japan, Apr. 2024, pp. 298–301.
- [8] M. Mirmozafari, G. Zhang, C. Fulton and R. J. Doviak, “Dual-polarization antennas with high isolation and polarization purity: A review and comparison of cross-coupling mechanisms”, *IEEE Antennas Propag. Mag.*, vol. 61, no. 1, pp. 50–63, Feb. 2019.
- [9] S. X. Ta, D. M. Nguyen, K. K. Nguyen, C. Dao-Ngoc and N. Nguyen-Trong, “Dual-Polarized Omnidirectional Antenna With Simple Feed and Ultrawide Bandwidth,” *IEEE Antennas Wireless Propag. Lett.*, vol. 19, no. 5, pp. 871–875, May 2020.
- [10] X. Zhai, S. Yan, B. Wang, and J. Zhang, “A Low-Profile Broadband Dual-Polarized Omnidirectional Antenna for LTE Applications,” *IEEE Antennas Wireless Propag. Lett.*, vol. 22, no. 7, pp. 1696–1700, Jul. 2023.
- [11] J. Zhou, Y.-H. Ke, and J.-X. Chen, “A Dual-Polarized Omnidirectional Antenna With Small Plane Size for Indoor Distribution Applications,” *IEEE Antennas Wireless Propag. Lett.*, vol. 22, no. 8, pp. 1878–1882, Aug. 2023.
- [12] J. D. Peng, Q. D. Liu, L. H. Ye, X.-X. Tian, J.-F. Li, D.-L. Wu and X. Y. Zhang, “Low-Profile Ultra-Wideband Dual-Polarized Omnidirectional Antenna for Indoor Base Station,” *IEEE Trans. Antennas Propag.*, vol. 71, no. 9, pp. 7597–7602, Sep. 2023.
- [13] P. F. Hu, K. W. Leung, Y. M. Pan, and S. Y. Zheng, “A Tri-Band Dual-Polarized Omnidirectional Dielectric Resonator Antenna With a Planar Feed for Indoor Applications,” *IEEE Trans. Antennas Propag.*, vol. 72, no. 1, pp. 401–411, Jan. 2024.
- [14] Z. Wang, T. Liang, and Y. Dong, “Compact In-Band Full Duplexing Antenna for Sub-6 GHz 5G Applications,” *IEEE Antennas Wireless Propag. Lett.*, vol. 20, no. 5, pp. 683–687, May 2021.
- [15] Y. Zhang, P. Liu, Y. Yin, and Y. Li, “Omnidirectional Dual-Polarized Antenna Using Collocated Slots With Wedgy Profile,” *IEEE Trans. Antennas Propag.*, vol. 69, no. 9, pp. 5446–5454, Sep. 2021.
- [16] T. Mizutani, N. Michishita, H. Sato, Y. Koyanagi, and H. Morishita, “Increasing bandwidth of orthogonally polarised omnidirectional antenna composed of halo and sleeve antennas,” *IET Microw. Antennas Propag.*, vol. 17, no. 7, pp. 565–573, 2023.
- [17] Y. Zhang, Y. Li, W. Zhang, Z. Zhang, and Z. Feng, “Omnidirectional Antenna Diversity System for High-Speed Onboard Communication,” *Engineering*, vol. 11, pp. 72–79, Apr. 2022.